3. Annual report of project:

3.1 Project title

***In silico* analyses for interaction of persistent organic pollutants with constitutive androstane receptor**.

3.2. Members of project

Name	Affiliation
Pham Thi Dau	Department of Ecology, Faculty of Biology VNU University of Science, Vietnam National University, Hanoi, Vietnam
Masashi Hirano	Department of Biological and Chemical Systems Engineering, National Institute of Technology, Kumamoto College, Japan
Hisato Iwata	Lab. of Environmental Toxicology, Center for Marine Environmental Studies, Ehime University, Japan

3.3. Results of project:

3.3.1. Aim of research:

In silico analysis for the interaction of CAR proteins with POPs to understand the structure-activity relationship of POPs and molecular mechanism (binding mode) of POP-CAR interaction.

3.3.2. Procedure:

- Step 1: Constructed the homology model of CAR LBD proteins from Baikal seal and mouse:

The homology modeling for the CAR LBDs were performed using the programs of Molecular Operating Environment (MOE) (Chemical Computing Group Inc., Montreal, QB, Canada). The crystal structures of hCAR and mCAR LBDs were obtained from Protein Data Bank (PDB) entry 1xvp (Xu *et al*., 2004) and 1xls (Suino *et al*., 2004), respectively. The crystal structure of hCAR has been constructed based on CAR/RXR LBD heterodimer bound to CITCO and a SRC1 peptide and that of mCAR has been based on CAR/RXR LBD heterodimer bound to TCPOBOP and 9cis-retinoic acid and a TIF2 peptide. To build a homology model of bsCAR LBD, 1xvp was taken as a template. The amino acid sequence of bsCAR LBD was aligned with that of 1xvp to yield a readily superimposable three-dimensional model. The structure of bsCAR LBD in the absence of the ligand was optimized by AMBER99 force field with an energy gradient of 0.05 (Wang *et al*., 2000).

- Step 2: Establish the structure of POPs, including PCBs and PBDEs

Chemical structures were drawn by Symyx Draw ver. 4.0

- Step 3: Analyze the interaction of each compound with each CAR protein

The obtained models of bsCAR and mCAR LBDs were prepared with Protonate 3D program by adjusting the protonation state to pH 7.0 of the running buffer in which the ligand-CAR interaction was monitored. These structures were then used to identify the ligand-binding sites using MOE Alpha Site Finder. Chemical structures were constructed using the

ISIS/Draw program (MDL Information Systems Inc., San Leandro, CA) and rendered and minimized with the MMFF94x force field in MOE (Halgren, 1996). To calculate the molecular volume of some tested chemicals in aqueous phase, molecular dynamics (MD) experiments were conducted using the MMFF94x force field with gas-phase electrostatics. For MD simulations, the Nose-Hoover-Andersen method was used as a NVT ensemble. The systems were subjected to 20 ps heating and equilibration from 100 to 300 K, followed by 1 ns simulation at 300 K with 2 fs time steps. The molecular volumes of the resulting ligand structures were calculated by the AtomRegion program using a grid space of 0.1 Å. The possible docking of POPs were searched with the NormalDock program. All the algorithms of NormalDock were coded using MOE's powerful vector language SVL (Scientific Vector Language). Existing features implemented in MOE were fully applied to realize the functions of NormalDock. A total of 250 conformations for each chemical were generated by Lowmode MD. The ligand conformations were subjected to energy minimization using MMFF94x force field.

- Step 4: Compare the binding potencies (interaction energies) of POPs with CAR and identify the amino acid residues participating in the binding with POPs

The most stable binding modes of ligands with the CARs were determined on the basis of the lowest S-score value (kcal/mol). The critical amino acids for the ligand interaction were determined by the ligand interaction module of MOE

- Step 5: Explain the difference in the response of CARs to POPs based on the structure, interaction energy, and binding mode.

3.3.3. Results:

3.3.3.1. The homology model of CAR LBDs

The sequence alignment of CAR LBDs were compared using MacVector software (Fig. 1). These sequences were used to construct the homology model of CAR LBDs.

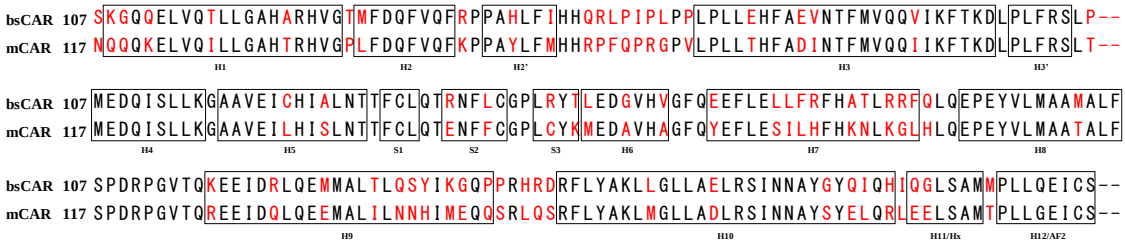

Figure 1: Sequence alignment of bsCAR and mCAR LBD. Different residues between mCAR with bsCAR LBD are red characters

To construct a homology model for bsCAR LBD, we applied a crystal structure of hCAR LBD as a template (Xu *et al*., 2004) because they share a 84% amino acid identity (Sakai *et al*., 2006). The homology model of bsCAR LBD bears a close resemblance to hCAR LBD, with a low root-mean square deviation (RMSD) value (0.408Å). The structure of bsCAR LBD was also compared with mCAR LBD (Fig. 2).

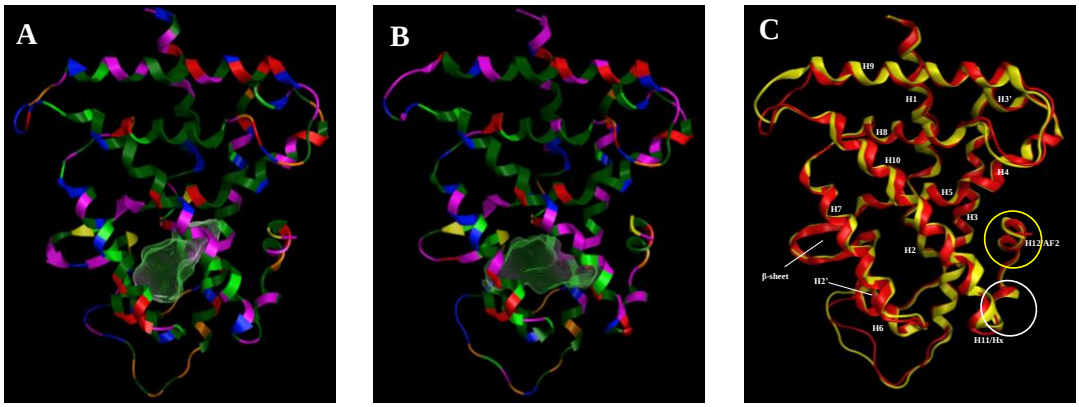

Figure 2: The homology modeling of (A) bsCAR LBD and (B) mCAR LBD. (C) Structural comparison between bsCAR LBD and mCAR LBD. bsCAR is colored in red and mCAR is in yellow, and structural elements are noted. LBD structures with LBP of bsCAR (magenta net) and mCAR (white net) were calculated with MOE Atom Region option. The *circle* indicates the helix 11 (white) and 12 (yellow) that are involved in the dimerization and transactivation of CAR, respectively.

The results revealed that bsCAR LBD (Fig. 2A) had a similar secondary structure with mCAR LBD (Fig. 2B), including eleven α helices, two 3^{10} helices (H2 and H2′), and three small β strands (Fig 2C). LBD of bsCAR displayed a short linker region (H11/Hx) between helices H10 and H12/AF2 and also a short H12/AF2 helix. The ligand-binding sites and/or ligand-binding pocket (LBP) of mCAR and bsCAR were determined using the MOE Alpha Site Finder. The structural comparison of mCAR and bsCAR was made in the apo structure. The result showed that bsCAR has an almost equal size of the LBP volume as mCAR (666 $Å^3$ for bsCAR and 656 $Å^3$ for mCAR). The LBPs were mainly constituted by hydrophobic residues and only a few hydrophilic residues that belong to helices H3, H4, H5, H6, H7, and H10 and two beta sheets, S2 and S3. The linker helix 11 (helix X) and helix 12 covered one side of the pocket. The main difference between bsCAR and mCAR LBDs was observed in loop regions.

3.3.3.2. The structure of PCBs and PBDEs

The 2D structures of PCBs (Fig. 3) and PBDEs (Fig 4) were drawn using Symyx Draw ver. 4.0 for the in silico analysis for the interaction with CAR LBDs.

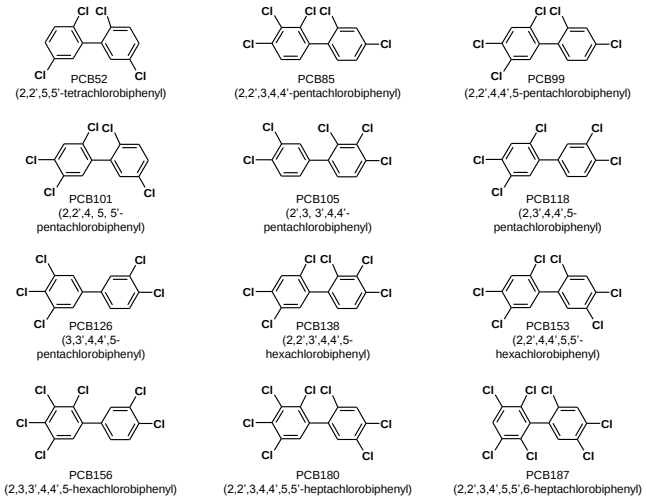

Figure 3: The 2D structures of PCBs were drawn using Symyx Draw ver 4.0.

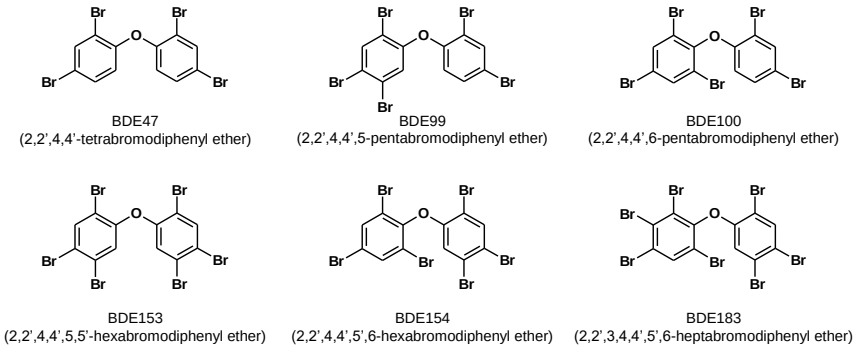

Figure 4: The 2D structures of PBDEs were drawn using Symyx Draw ver 4.0.

3.3.3.3. The interaction of POPs with each CAR LBDs

To understand the molecular basis of differences in the binding of POPs to CAR LBDs, we compared the *in silico* binding scores (S-score) for the interaction of each POPs with bsCAR and mCAR (Fig. 5). Results revealed that the binding potencies (S-scores) with POPs were similar between bsCAR and mCAR. However, the binding energy (S-scores) with CAR of PBDEs seem to be higher than that of PCBs.

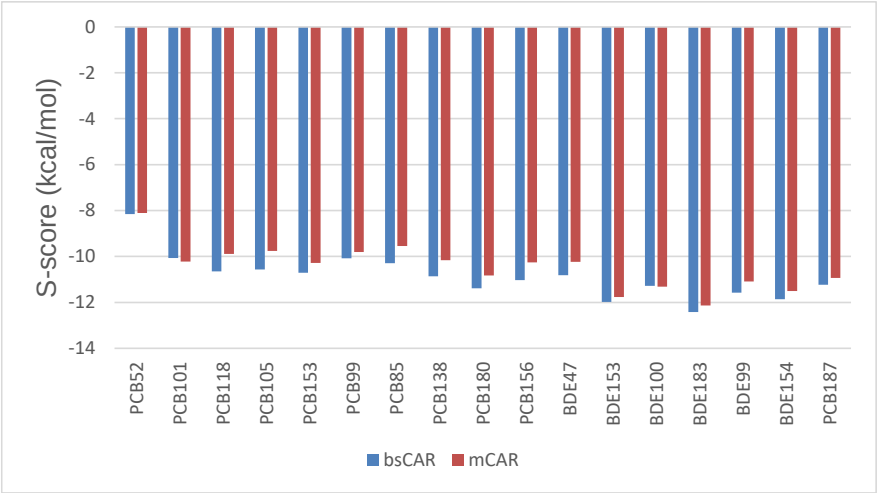

Figure 5: The free energy of binding between pollutants and predicted models (bsCAR and mCAR from Normal-Docking program using MOE software.

We also compared between the S-scores of POPs determined using *in silico* docking simulations (CAR LBDs) and their relative binding potencies (RBPs) determined using *in vitro* CAR binding assays (Fig 6A and 6B).

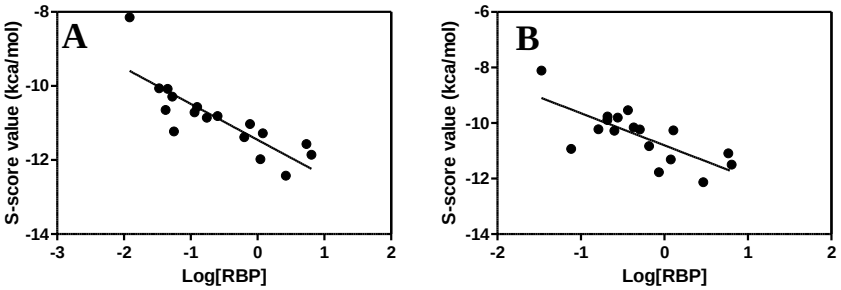

Figure 6: Relationships between the free energy (S-score) and their relative binding potencies (RBPs) to the (A) Baikal seal CAR LBD and (B) mouse CAR LBD.

The results revealed the significant negative correlation between the S-scores of POPs for bsCAR LBD (r = -0.8298, p < 0.001) and mCAR LBD (r = -0.7379, p < 0.001) with their RBPs. These results suggested that *in silico* docking simulation may be a useful tool for screening potential ligands for CAR LBPs.

Finally, the critical amino acids for the ligand interaction were determined by the ligand interaction module of MOE (Fig 7). The ligands are oriented toward the beta sheet 3(S3) of bsCAR (orange region), and toward the helix 10 in mCAR (blue region). Thus, the regions of binding are slightly different between bsCAR and mCAR.

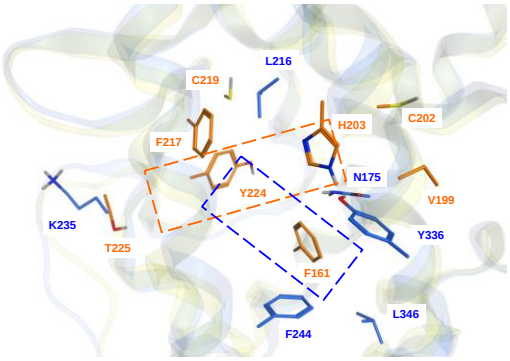

Figure 6: Superimpose of the important amino acids in bsCAR (orange) and mCAR (blue) LBD.

PLIF analysis showed that there were difference in binding between PBDEs and PCBs (Fig. 7). Because, in bsCAR, Thr225 and Cys219 have been interacting with PBDEs, whereas PCBs interacts with only Thr225. In mCAR, Tyr336 interacts mostly with PBDEs.

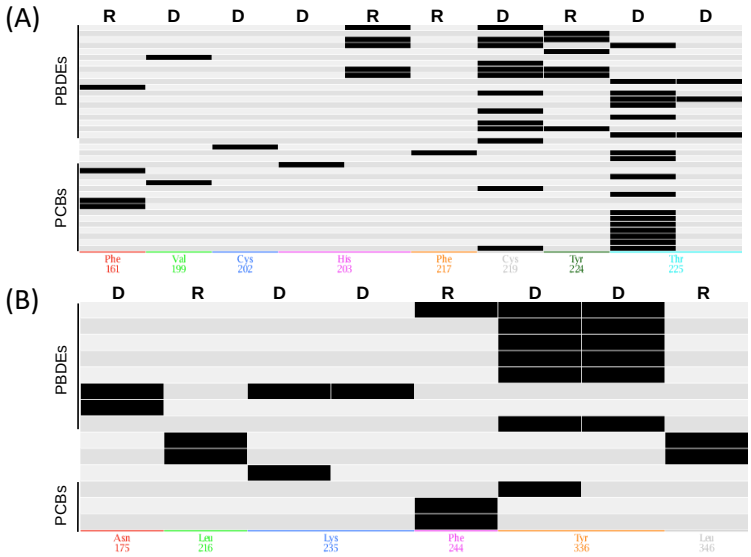

Figure 7: Barcode display analysis of PLIF results for LBDs of bsCAR (A) and mCAR (B). The horizontal rods correspond to each of the studied compounds. A black rod indicates the presence of an interaction with residues shown in the X-axis at the bottom of each graph. D and R denotes the donor and π-stacking interactions, respectively.

3.3.4. Perspectives in future:

Write a manuscript to be submitted to an international journal.